Use this document as a template

Millikelvin Confocal Microscopy of Semiconductor Membranes and Filter Functions for Unital Quantum Operations

Customise this page according to your needs

Tobias Hangleiter*

September 4, 2025

* A LaTeX lover/hater

The harmony of the world is made manifest in Form and Number, and the heart and soul and all the poetry of Natural Philosophy are embodied in the concept of mathematical beauty.

– D'Arcy Wentworth Thompson

Contents

List of Figures

Part I

A Flexible Python Tool For Fourier-Transform Noise Spectroscopy

Part II

Characterization and Improvements of a Millikelvin Confocal Microscope

Part III

Optical Measurements of Electrostatic Exciton Traps in Semiconductor Membranes

Part IV

A Filter-Function Formalism For Unital Quantum Operations

Appendix

Filter Functions

A.1 Additional derivations

In this appendix we show additional derivations omitted from the main text.

A.1.1 Derivation of the single-qubit cumulant function in the Liouville representation

For a single qubit, the Pauli basis $\{\sigma_i\}_{i=0}^3 = 1/\sqrt{2}\times\{\mathbb{1}, \sigma_x, \sigma_y, \sigma_z\}$ is a natural choice to define the Liouville representation. In this case, the trace tensor **??** can be simplified and thus **??** given a more intuitive form which we derive in this appendix. Since the cumulant function is linear in the noise indices α, β we drop them in the following for legibility. Our results hold for both a single pair of noise indices and the total cumulant. We start by observing the relation

$$T_{klij} = \mathrm{tr}\big(\sigma_k\sigma_l\sigma_i\sigma_j\big) = \frac{1}{2}(\delta_{kl}\delta_{ij} - \delta_{ki}\delta_{lj} + \delta_{kj}\delta_{li}) \tag{A.1}$$

for the Pauli basis elements $\sigma_k, k \in \{1, 2, 3\}$. Including the identity element σ_0 in the trace tensor gives additional terms. However, as we show now none of these contribute to $\mathcal{K}$ because they cancel out.

First, since the noise Hamiltonian $H_\mathrm{n}(t)$ is traceless and therefore $\tilde{\mathcal{B}}_{\alpha 0}(t) = 0$, we have $\Gamma_{kl}, \Delta_{kl} \propto (1-\delta_{k0})(1-\delta_{0l})$, *i.e.* the first column and row of both the decay amplitude and frequency shift matrices are zero, and hence terms in the sum of **??** with either $k = 0$ or $l = 0$ vanish. Next, for $i = j = 0$ all of the traces cancel out as can be easily seen. The last possible cases are given by $i = 0, j \neq 0$ and vice versa. For these cases we have

$$T_{kl0j} = T_{klj0} = \frac{1}{\sqrt{2}}\,\mathrm{tr}\big(\sigma_k\sigma_l\sigma_j\big) = \frac{i}{2}\varepsilon_{klj} \tag{A.2}$$

with ε_{klj} the completely antisymmetric tensor. Both of the above cases vanish in $\mathcal{K}$ since, taking the case $j = 0$ for example,

$$\frac{1}{2}\left(T_{kl0i} - T_{k0li} - T_{kil0} + T_{ki0l}\right) = \frac{i}{2}\left(\varepsilon_{kli} - \varepsilon_{kli} - \varepsilon_{kil} + \varepsilon_{kil}\right) = 0 \tag{A.3a}$$

for the decay amplitudes Γ and

$$\frac{1}{2}\left(T_{kl0i} - T_{lk0i} - T_{kli0} + T_{lki0}\right) = \frac{i}{2}\left(\varepsilon_{kli} - \varepsilon_{lki} - \varepsilon_{kli} + \varepsilon_{lki}\right) = 0 \tag{A.3b}$$

for the frequency shifts Δ. Hence, only terms with $i, j > 0$ contribute and we can plug the simplified expressions for the trace tensor T_{klij}, Equation A.1, into **??** to write the cumulant function for a single qubit and the

Pauli basis concisely as

$$\mathcal{K}_{ij}(\tau) = -\frac{1}{2}\sum_{kl}\Big[\Delta_{kl}\left(T_{klji} - T_{lkji} - T_{klij} + T_{lkij}\right) + \Gamma_{kl}\left(T_{klji} - T_{kjli} - T_{kilj} + T_{kijl}\right)\Big] \tag{A.4}$$

$$= -\sum_{kl}\left[\Delta_{kl}(\delta_{ki}\delta_{lj} - \delta_{kj}\delta_{li}) + \Gamma_{kl}(\delta_{kl}\delta_{ij} - \delta_{kj}\delta_{li})\right] \tag{A.5}$$

$$= \Delta_{ji} - \Delta_{ij} + \Gamma_{ij} - \delta_{ij}\operatorname{tr}\Gamma \tag{A.6}$$

$$= \begin{cases} -\sum_{k\neq i}\Gamma_{kk} & \text{if} \quad i = j, \\ -\Delta_{ij} + \Delta_{ji} + \Gamma_{ij} & \text{if} \quad i \neq j, \end{cases} \tag{A.7}$$

as given in the main text.

A.1.2 Evaluation of the integrals in ??

Here we calculate the integrals appearing in the calculation of the frequency shifts Δ, **??**, given by

$$I^{(g)}_{ijmn}(\omega) = \int_{t_{g-1}}^{t_g} \mathrm{d}t\, e^{i\Omega^{(g)}_{ij}(t-t_{g-1})-i\omega t}\int_{t_{g-1}}^{t} \mathrm{d}t'\, e^{i\Omega^{(g)}_{mn}(t'-t_{g-1})+i\omega t'}. \tag{A.8}$$

The inner integration is simple to perform and we get

$$I^{(g)}_{ijmn}(\omega) = \int_{t_{g-1}}^{t_g} \mathrm{d}t\, e^{i\Omega^{(g)}_{ij}(t-t_{g-1})-i\omega(t-t_{g-1})} \times \begin{cases} \dfrac{e^{i(\omega+\Omega^{(g)}_{mn})(t-t_{g-1})}-1}{i(\omega+\Omega^{(g)}_{mn})} & \text{if} \quad \omega+\Omega^{(g)}_{mn} \neq 0 \\ t - t_{g-1} & \text{if} \quad \omega+\Omega^{(g)}_{mn} = 0. \end{cases} \tag{A.9}$$

Shifting the limits of integration and performing integration by parts in the case $\omega + \Omega^{(g)}_{mn} = 0$ then yields

$$I^{(g)}_{ijmn}(\omega) = \tag{A.10}$$
$$\begin{cases} \frac{1}{\omega+\Omega^{(g)}_{mn}}\left(\frac{e^{i(\Omega^{(g)}_{ij}-\omega)\Delta t_g}-1}{\Omega^{(g)}_{ij}-\omega} - \frac{e^{i(\Omega^{(g)}_{ij}+\Omega^{(g)}_{mn})\Delta t_g}-1}{\Omega^{(g)}_{ij}+\Omega^{(g)}_{mn}}\right) & \text{if } \omega+\Omega^{(g)}_{mn} \neq 0, \\ \frac{1}{\Omega^{(g)}_{ij}-\omega}\left(\frac{e^{i(\Omega^{(g)}_{ij}-\omega)\Delta t_g}-1}{\Omega^{(g)}_{ij}-\omega} - i\Delta t_g e^{i(\Omega^{(g)}_{ij}-\omega)\Delta t_g}\right) & \text{if } \omega+\Omega^{(g)}_{mn} = 0 \wedge \Omega^{(g)}_{ij}-\omega \neq 0, \\ \frac{\Delta t_g^2}{2} & \text{if } \omega+\Omega^{(g)}_{mn} = 0 \wedge \Omega^{(g)}_{ij}-\omega = 0. \end{cases}$$

A.1.3 Simplifying the calculation of the entanglement infidelity

In the main text, we claimed that the contribution of noise sources (α, β) to the total entanglement infidelity $I_{\text{ent}}(\tilde{\mathcal{U}}) = \sum_{\alpha\beta} I_{\alpha\beta}$ reduces from the trace of the cumulant function $\mathcal{K}$ to

$$I_{\alpha\beta} = -\frac{1}{d^2}\operatorname{tr}\mathcal{K}_{\alpha\beta} \tag{A.11}$$

$$= \frac{1}{d}\operatorname{tr}\Gamma_{\alpha\beta}. \tag{A.12}$$

To show this, we substitute $\mathcal{K}$ by its definition in terms of Δ and Γ according to **??**. This yields for the trace

$$\begin{aligned}\operatorname{tr}\mathcal{K}_{\alpha\beta} &= -\frac{1}{2}\sum_{kl}\delta_{ij}(f_{ijkl}\Delta_{\alpha\beta,kl} + g_{ijkl}\Gamma_{\alpha\beta,kl}) \\ &= -\frac{1}{2}\sum_{ikl}\Gamma_{\alpha\beta,kl}\left(T_{klii} + T_{lkii} - 2T_{kili}\right)\end{aligned} \tag{A.13}$$

since Δ is antisymmetric. In order to further simplify the trace tensors on the right hand side of Equation A.13, we observe that the orthonormality and completeness of the operator basis C defining the Liouville representation of $\mathcal{K}$ (*cf.* **??**) is equivalent to requiring that $\mathsf{C}^\dagger\mathsf{C} = \mathbb{1}$ with C reshaped into a $d^2 \times d^2$ matrix by a suitable mapping. This condition may also be written as

$$\begin{aligned}\delta_{ac}\delta_{bd} &= \sum_k C^*_{k,ab}C_{k,cd} \\ &= \sum_k C_{k,ba}C_{k,cd}\end{aligned} \tag{A.14}$$

because every element C_k is Hermitian. Using this relation in Equation A.13 then yields

$$\begin{aligned}\operatorname{tr}\mathcal{K}_{\alpha\beta} &= -\frac{1}{2}\sum_{kl}\Gamma_{\alpha\beta,kl}\left(2d\delta_{kl} - 2\operatorname{tr}(C_k)\operatorname{tr}(C_l)\right) \\ &= -d\operatorname{tr}\Gamma_{\alpha\beta}.\end{aligned} \tag{A.15}$$

The last equality only holds true for bases with a single non-traceless element (the identity), such as the bases discussed in **??**. This is because in this case, $\operatorname{tr}(C_k) = 0$ for $k > 0$ whereas $\Gamma_{\alpha\beta,kl} = 0$ for either $k = 0$ or $l = 0$ since Γ is a function of the traceless noise Hamiltonian for which $\operatorname{tr}(C_0 H_\mathrm{n}) \propto \operatorname{tr} H_\mathrm{n} = 0$ (*i.e.* the first column of the control matrix is zero, see **????**). Finally, substituting Equation A.15 into Equation A.11 we obtain our result

$$I_{\alpha\beta} = \frac{1}{d}\operatorname{tr}\Gamma_{\alpha\beta}. \tag{A.16}$$

A.1.4 Sum rule

For white noise, the infidelity to leading order does not depend on the internal dynamics of the control operation but only on the total duration τ. To see this, take **??** and substitute the correlation function of white noise, $\langle b_\alpha(t_1)b_\alpha(t_2)\rangle = S_0\delta(t_1 - t_2)$. The integrals then simplify to

$$\Gamma_{\alpha\alpha,kl} = S_0\int_0^\tau \mathrm{d}t\,\tilde{\mathcal{B}}_{\alpha k}(t)\tilde{\mathcal{B}}_{\alpha l}(t). \tag{A.17}$$

In order to compute the infidelity, we require the trace over the matrix of decay amplitudes (**??**), so

$$I_\alpha = \frac{S_0}{d}\operatorname{tr}\Gamma_{\alpha\alpha} = \frac{1}{d}\sum_k\int_0^\tau \mathrm{d}t\,\tilde{\mathcal{B}}^2_{\alpha k}(t). \tag{A.18}$$

Now recall that $\tilde{\mathcal{B}}$ is a vector on Liouville space and we can write $\tilde{\mathcal{B}}_\alpha(t) \doteq |\tilde{B}_\alpha(t)\rangle\!\rangle \equiv \langle\!\langle\tilde{B}_\alpha(t)|$ because it is Hermitian. Thus,

$$I_\alpha = \frac{S_0}{d}\int_0^\tau \mathrm{d}t\,\langle\!\langle\tilde{B}_\alpha(t)|\tilde{B}_\alpha(t)\rangle\!\rangle = \frac{1}{d}\int_0^\tau \mathrm{d}t\,\left\|\tilde{B}_\alpha(t)\right\|^2, \tag{A.19}$$

and if $B_\alpha(t) = B_\alpha$, *i.e.*, is time-independent, the integral evaluates simply to τ,

$$I_\alpha = \frac{S_0\tau}{d}\left\|\tilde{B}_\alpha\right\|^2, \tag{A.20}$$

because the control unitary $U_c(t)$ conserves the norm. Since also $I_\alpha = \int \mathrm{d}\omega/2\pi d\, S(\omega)\mathcal{F}_\alpha(\omega)$ with the fidelity filter function $\mathcal{F}_\alpha(\omega)$ (**????**), this result also implies the sum rule

$$\int \frac{\mathrm{d}\omega}{2\pi}\mathcal{F}_\alpha(\omega) = \tau\left\|\tilde{B}_\alpha\right\|^2, \tag{A.21}$$

a result previously obtained by Cywiński et al. [1]. This means that pulse shaping and similar techniques never yield a leading-order fidelity enhancement if the noise is white in the relevant regime of frequencies as the fidelity only depends on the total duration of the pulse.

A.2 Singlet-Triplet Gate Fidelity

In this appendix we lay out in more detail how the fidelity of the optimized S-T_0 qubit gates from Reference 2 was calculated using filter functions. In two singlet-triplet qubits, angular momentum conservation suppresses occupancy of states with non-vanishing magnetic spin quantum number m_s so that the total accessible state space of dimension $d = 6$ is spanned by $\{|\uparrow\downarrow\uparrow\downarrow\rangle, |\uparrow\downarrow\downarrow\uparrow\rangle, |\downarrow\uparrow\uparrow\downarrow\rangle, |\downarrow\uparrow\downarrow\uparrow\rangle, |\uparrow\uparrow\downarrow\downarrow\rangle, |\downarrow\downarrow\uparrow\uparrow\rangle\}$. A straightforward method to single out the computational subspace (CS) dynamics from those on the whole space would be to simply project the error transfer matrix $\tilde{\mathcal{U}} \approx \mathbb{1} + \mathcal{K}$ with $\mathcal{K}$ the cumulant function onto the CS as proposed by Wood and Gambetta [3], that is calculate the fidelity as $F_{\mathrm{ent}} = d_c^{-2}\mathrm{tr}\big(\Pi_c\tilde{\mathcal{U}}\big)$ where Π_c is the Liouville representation of the projector onto the CS and $d_c = 4$ the dimension of the CS. However, here we use a more involved procedure in order to gain more insight from the error transfer matrix as well as to obtain a better comparison to the fidelities computed by Cerfontaine et al. [2], who map the final 6×6 propagator to the closest unitary on the 4×4 CS during their Monte Carlo simulation.

To calculate the fidelity of the target unitary on the 4×4 CS, we thus construct an orthonormal operator basis C of the full 6×6 space that is partitioned into elements which are nontrivial only on the CS on the one hand and elements which are nontrivial only on the remaining space on the other such that $\mathsf{C} = \mathsf{C}^c \cup \mathsf{C}^\ell$. Using such a basis, we can then trace only over CS elements of the error transfer matrix $\tilde{\mathcal{U}}$ in **??** to obtain the fidelity of the gate on the CS. Moreover, we retain the opportunity to characterize the gates on the basis of the Pauli matrices.

Since there is no obvious way to extend the Pauli basis for two qubits to the complete space we proceed as follows: For the CS, we pad the two-qubit Pauli basis with zeros on the leakage levels, *i.e.*

$$C_i^c \doteq \begin{array}{c} \\ \langle\uparrow\uparrow\downarrow\downarrow| \\ \langle\downarrow\downarrow\uparrow\uparrow| \end{array} \begin{array}{c} \begin{array}{ccc} |\uparrow\uparrow\downarrow\downarrow\rangle & & |\downarrow\downarrow\uparrow\uparrow\rangle \end{array} \\ \begin{pmatrix} P_i & 0 & 0 \\ 0 & 0 & 0 \\ 0 & 0 & 0 \end{pmatrix} \end{array}, \quad i \in \{0, \dots, 15\}, \tag{A.22}$$

where the P_i are normalized two-qubit Pauli matrices (*cf.* **??**) in the basis $\{|\uparrow\downarrow\uparrow\downarrow\rangle, |\uparrow\downarrow\downarrow\uparrow\rangle, |\downarrow\uparrow\uparrow\downarrow\rangle, |\downarrow\uparrow\downarrow\uparrow\rangle\}$. To complete the basis we require an additional 20 elements orthogonal to the 16 padded Pauli matrices. We

obtain the remaining elements by first expanding the C_i^c in an arbitrary basis $\{\Lambda_i\}_{i=0}^{35}$ of the complete space (we choose a generalized Gell-Mann (GGM) basis, **??**, for simplicity), yielding a 16×36 matrix of expansion coefficients:

$$M_{ij} = \mathrm{tr}\big(C_i^c \Lambda_j\big). \tag{A.23}$$

We then compute an orthonormal vector basis V (a matrix of size 36×20) for the null space of M using singular value decomposition $M = U\Sigma V^\dagger$ and acquire the corresponding basis matrices as

$$C_i^\ell = \sum_j \Lambda_j V_{ji}, \quad i \in \{0, \ldots, 19\}. \tag{A.24}$$

Finally, to account for the fact that Reference 2 map the total propagator to the closest unitary on the CS, we exclude the identity Pauli element $C_0^c \propto \mathrm{diag}(1,1,1,1,0,0)$ from the trace over the computational subspace part of $\tilde{\mathcal{U}}$ represented in the basis $\mathsf{C} = \mathsf{C}^c \cup \mathsf{C}^\ell$ when calculating the fidelity,

$$F_{\mathrm{ent}} = \frac{1}{16} \sum_{i=1}^{15} \tilde{\mathcal{U}}_{ii}, \tag{A.25}$$

since for unitary operations on the CS we have $\mathcal{K}_{00} \approx 1 - \tilde{\mathcal{U}}_{00} = 1 - \mathrm{tr}\big(C_0^c \tilde{U} C_0^c \tilde{U}^\dagger\big) = 0$. Hence, excluding $\tilde{\mathcal{U}}_{00}$ from the trace corresponds to partially disregarding non-unitary components of the error channel on the computational subspace. Although not the only element that differs compared to the closest subspace unitary, $\mathcal{K}_{00}$ contains the most obvious contribution, whereas those of other elements are more difficult to disentangle into unitary and non-unitary components.

Similar to the fidelity, we also obtain the canonical filter function shown in panel (b) of **??** by summing only over columns one through 15 of the control matrix, $F_{\epsilon_{ij}}(\omega) = \sum_{k=1}^{15} \big|\tilde{\mathcal{B}}_{\epsilon_{ij}k}(\omega)\big|^2$. In fact, including the first column, corresponding to the padded identity matrix C_0^c, in the filter function removes the DCG character of $F_{\epsilon_{12}}(\omega)$ and $F_{\epsilon_{34}}(\omega)$, which instead approach a constant level of around 20 (note that the filter function is dimensionless in our units) at zero frequency. This is consistent with the fact that the gates were optimized using quasistatic and fast white noise contributions to the fidelity after mapping to the closest unitary on the computational subspace. We have performed Monte Carlo resimulations that support this reading. In Figure A.1 we show the filter functions once including and once excluding the contributions from C_0^c.

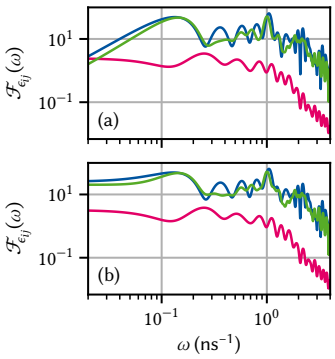

Figure A.1: Filter functions of the voltage detunings ϵ_{ij} excluding (a) and including (b) the zero-padded identity matrix basis element $C_0^c \propto \mathrm{diag}(1,1,1,1,0,0)$ for the computational subspace. Evidently, including C_0^c removes the dynamically corrected gate (DCG) character, namely that $F_{\epsilon_{ij}}(\omega) \to 0$ as $\omega \to 0$, of the gates but has little effect on the high-frequency behavior. As the pulse optimization minimizes, among other figures of merit, the infidelity of the final propagator mapped to the closest unitary on the computational subspace due to quasistatic and fast white noise, this indicates that excluding C_0^c from the filter function corresponds to partially neglecting non-unitary components of the propagator on the computational subspace.

A.3 GRAPE-optimized gate set for QFT

For completeness, in this appendix we give details on the GRAPE-optimized pulses for the gate set $\mathbb{G} = \{\mathrm{X}_i(\pi/2), \mathrm{Y}_i(\pi/2), \mathrm{CR}_{ij}(\pi/2^3)\}$ used in **??** to simulate a quantum Fourier transform (QFT) algorithm. As mentioned in the main text, we consider a toy Rabi driving model with in-phase/quadrature (IQ) single-qubit control and exchange to mediate inter-qubit coupling. Cast in the language of quantum optimal control theory this translates to a vanishing drift (static) Hamiltonian, $H_\mathrm{d} = 0$, and a control Hamiltonian

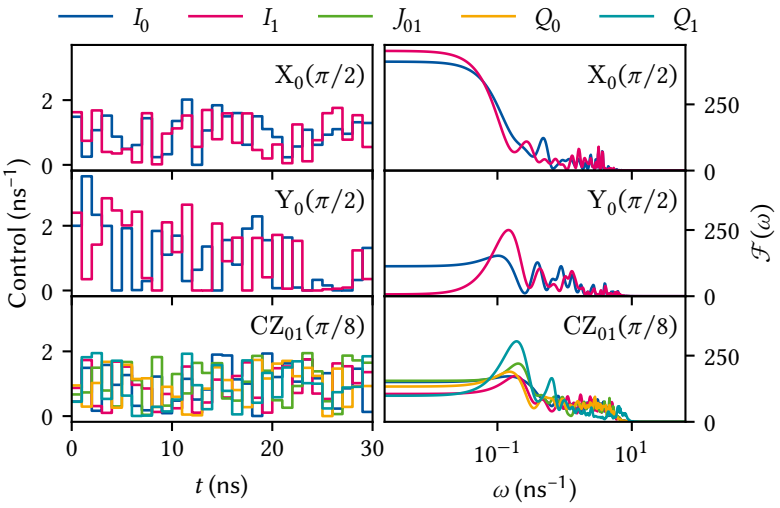

Figure A.2: Control fields (top row) and corresponding filter functions (bottom row) of the gradient ascent pulse engineering (GRAPE)-optimized pulses in G. (a),(b) $X_0(\pi/2)$; (c),(d) $Y_0(\pi/2)$; (e),(f) $CR_{01}(\pi/2^3)$. Note that the optimization is neither very sophisticated nor realistic as the algorithm only maximizes the systematic (coherent) fidelity $\mathrm{tr}(UQ_{\mathrm{targ}}^{\dagger})/d$ and the randomly distributed initial control amplitudes are not subject to any constraints.

in the rotating frame given by

$$H_{\mathrm{c}}(t) = H_{\mathrm{c}}^{(0)}(t) \otimes \mathbb{1} + \mathbb{1} \otimes H_{\mathrm{c}}^{(1)}(t) + H_{\mathrm{c}}^{(01)}(t), \tag{A.26}$$

$$H_{\mathrm{c}}^{(i)}(t) = I_i(t)\sigma_x^{(i)} + Q_i(t)\sigma_y^{(i)}, \tag{A.27}$$

$$H_{\mathrm{c}}^{(ij)}(t) = J_{ij}(t)\sigma_z^{(i)} \otimes \sigma_z^{(j)}, \tag{A.28}$$

where $I_i(t)$ and $Q_i(t)$ are the in-phase and quadrature pulse envelopes and $\sigma_{x,y}^{(i)}$ are the Pauli matrices acting on the ith and extended trivially to the other qubit. As our goal is only of illustrative nature and not to provide a detailed gate optimization, we obtain the controls $\{I_0(t), Q_0(t), I_1(t), Q_1(t), J_{12}(t)\}$ for the gate set $\mathbb{G}$ using the GRAPE algorithm implemented in `QuTiP` [4] initialized with randomly distributed amplitudes. The resulting pulses and the corresponding filter functions for the relevant noise operators are shown in Figure A.2.

A.4 Convergence Bounds

In this appendix we give bounds for the convergence of the expansions employed in the main text for the case of purely autocorrelated noise, $S_{\alpha\beta}(\omega) = \delta_{\alpha\beta}S_{\alpha\beta}(\omega) = S_{\alpha}(\omega)$, following the approach by Green et al. [5]. For Gaussian noise, our expansion is exact when including first and second order Magnus expansion (ME) terms. Hence, the convergence radius of the Magnus expansion (ME) becomes infinite and the fidelity can be computed exactly by evaluating the matrix exponential **??**. For non-Gaussian noise, the following considerations apply.

A.4.1 Magnus Expansion

The ME of the error propagator **??** converges if $\int_0^{\tau} \mathrm{d}t \|\tilde{H}_{\mathrm{n}}(t)\| < \pi$ with $\|A\|^2 = \langle A, A\rangle = \sum_{ij}|A_{ij}|^2$ the Frobenius norm [6]. We assume a time dependence of the noise operators of the form $B_{\alpha}(t) = s_{\alpha}(t)B_{\alpha}$. By the

Cauchy-Schwarz inequality we then have

$$\begin{aligned}\left\|\tilde{H}_{\mathrm{n}}(t)\right\|^2 &= \|H_{\mathrm{n}}(t)\|^2 \\ &= \sum_{\alpha\beta} s_\alpha(t)s_\beta(t)b_\alpha(t)b_\beta(t)\left\langle B_\alpha, B_\beta\right\rangle \\ &\leq \sum_{\alpha\beta} s_\alpha(t)s_\beta(t)b_\alpha(t)b_\beta(t)\|B_\alpha\|\,\|B_\beta\| \\ &\leq \left[\sum_\alpha \sum_{g=1}^{G} \vartheta^{(m)}(t)s_\alpha^{(m)}b_\alpha^{(m)}\|B_\alpha\|\right]^2\end{aligned} \tag{A.29}$$

where $b_\alpha^{(m)}$ is the maximum value that the noise assumes during the pulse, $\vartheta^{(g)}(t) = \theta(t-t_{g-1}) - \theta(t-t_g)$ is one during the gth time interval and zero else, and where we approximated the time evolution as piecewise constant. Then, in order to guarantee convergence of the ME,

$$\begin{aligned}\int_0^\tau \mathrm{d}t\,\|\tilde{H}_{\mathrm{n}}(t)\| &\leq \int_0^\tau \mathrm{d}t\left|\sum_\alpha \sum_{g=1}^{G} \vartheta^{(m)}(t)s_\alpha^{(m)}b_\alpha^{(m)}\|B_\alpha\|\right| \\ &= \sum_\alpha b_\alpha^{(m)}\|B_\alpha\| \sum_{g=1}^{G} s_\alpha^{(m)} \int_{t_{g-1}}^{t_g} \mathrm{d}t \\ &= \sum_\alpha C_m \delta b_\alpha \|B_\alpha\| \sum_{g=1}^{G} s_\alpha^{(m)}\Delta t_g \\ &=: N\end{aligned} \tag{A.30}$$

where we have expressed the in principle unknown maximum noise amplitude $b_\alpha^{(m)}$ in terms of the root mean square value δb_α. That is, $b_\alpha^{(m)} = C_m \langle b_\alpha(0)^2\rangle^{1/2} = C_m \delta b_\alpha$ for a sufficiently large value C_m. Finally, realizing that $\delta b_\alpha^2 = \int \frac{\mathrm{d}\omega}{2\pi} S_\alpha(\omega)$ and by the triangle inequality,

$$\begin{aligned}N &= C_m \sum_\alpha \|B_\alpha\| \left[\int_{-\infty}^{\infty} \frac{\mathrm{d}\omega}{2\pi} S_\alpha(\omega)\right]^{1/2} \sum_{g=1}^{G} s_\alpha^{(m)}\Delta t_g \\ &\leq C_m \left[\sum_\alpha \|B_\alpha\|^2 \int_{-\infty}^{\infty} \frac{\mathrm{d}\omega}{2\pi} S_\alpha(\omega)\left(\sum_{g=1}^{G} s_\alpha^{(m)}\Delta t_g\right)^2\right]^{1/2} \\ &=: C_m \xi \\ &\overset{!}{<} \pi\end{aligned} \tag{A.31}$$

where we have introduced the parameter ξ. Thus, the expansion converges if $\xi < \pi/C_m$. However, we note that in practice the rms noise amplitude δb_α will often be infinite, limiting the usefulness of this bound for certain noise spectra.

A.4.2 Infidelity

Again assuming a time dependence $B_\alpha(t) = s_\alpha(t)B_\alpha$ as well as piecewise-constant control, we note that for the infidelity we have (*cf.* **??**)

$$\begin{aligned}
|\mathrm{tr}(\Gamma)| &= \left|\sum_\alpha \int_0^\tau \mathrm{d}t_2 \int_0^\tau \mathrm{d}t_1 \,\langle b_\alpha(t_1) b_\alpha(t_2)\rangle \sum_k \tilde{\mathcal{B}}_{\alpha k}(t_1)\tilde{\mathcal{B}}_{\alpha k}(t_2)\right| \\
&\leq \left|\sum_\alpha \int_0^\tau \mathrm{d}t_2 \int_0^\tau \mathrm{d}t_1 \,\langle b_\alpha(t_1) b_\alpha(t_2)\rangle \sum_{g,g'=1}^{G} \vartheta^{(m)}(t_1)\vartheta^{(g')}(t_2) s_\alpha^{(m)} s_\alpha^{(g')} \|B_\alpha\|^2\right| \\
&\leq \sum_\alpha \|B_\alpha\|^2 \underbrace{\langle b_\alpha^2(0)\rangle}_{\int \frac{\mathrm{d}\omega}{2\pi} S_\alpha(\omega)} \sum_{g,g'=1}^{G} s_\alpha^{(m)} s_\alpha^{(g')} \left| \int_{t_{g'-1}}^{t_{g'}} \mathrm{d}t_2 \int_{t_{g-1}}^{t_g} \mathrm{d}t_1 \underbrace{\overline{\langle b_\alpha(t_1) b_\alpha(t_2)\rangle}}_{|\bullet|\leq 1} \right| \\
&\leq \sum_\alpha \left[\|B_\alpha\|^2 \int_{-\infty}^{\infty} \frac{\mathrm{d}\omega}{2\pi} S_\alpha(\omega) \left(\sum_{g=1}^{G} s_\alpha^{(m)} \Delta t_g \right)^2 \right] \\
&= \xi^2, \qquad \text{(A.32)}
\end{aligned}$$

where, going from the second to the third line, we have factored out the total power of noise source α from the cross-correlation function, $\langle b_\alpha(t_1) b_\alpha(t_2)\rangle = \langle b_\alpha^2(0)\rangle \left|\overline{\langle b_\alpha(t_1) b_\alpha(t_2)\rangle}\right|$. Thus, the first order infidelity **??** is upper-bounded by $d^{-1}\xi^2$, the same parameter also bounding the convergence of the ME, and higher orders can be neglected if $\xi^2 \ll 1$.

Note that similar arguments can be made for the higher orders of the ME [5]. In particular, the nth order ME term containing n-point correlation functions of the noise is of order $\mathcal{O}(\xi^n)$ as stated in the main text.

A.5 Second-order concatenation

In this appendix, I lay out how the second-order filter functions of atomic pulse segments can be re-used to compute the filter function of the concatenated sequence. While it is not possible, due to the nested time integral, to perform the calculation entirely without concern for the internal structure of the individual segments, it is also not necessary to compute everything from scratch.

refeq

We begin by setting some notation. Wherever possible, we omit indices and thus imply matrix multiplication between objects. We assume a single noise operator and drop the corresponding index; we can easily add them again later since none of the manipulations involve the noise indices. We fully adopt the picture that control matrices can be concatenated by summing over individual time steps, which may either be single piecewise-constant segments or entire sequences, corresponding to **??** or **??**, respectively. To make clear that the control "matrices" are in fact vectors in Liouville space, we write them as bras wherever possible,[1]

$$\tilde{\mathcal{B}}(\omega) \doteq \langle\!\langle \tilde{\mathcal{B}}(\omega)| \tag{A.33}$$

and define as shorthands for **??**

$$\mathcal{G}^{(g)}(\omega) \doteq \langle\!\langle \mathcal{G}^{(g)}(\omega)| \coloneqq e^{i\omega t_{g-1}} \langle\!\langle \tilde{\mathcal{B}}^{(g)}(\omega)|\, \mathcal{Q}^{(g-1)} \tag{A.34}$$

$$\mathcal{M}^{(g)}(\omega) \doteq \langle\!\langle \mathcal{M}^{(g)}(\omega)| \coloneqq \sum_{g'=1}^{g} \langle\!\langle \mathcal{G}^{(g')}(\omega)| \tag{A.35}$$

such that

$$\langle\!\langle \tilde{\mathcal{B}}(\omega)| = \langle\!\langle \mathcal{M}^{(G)}(\omega)| = \sum_{g'=1}^{G} \langle\!\langle \mathcal{G}^{(g')}(\omega)| \,. \tag{A.36}$$

I.e., $\mathcal{M}^{(g)}(\omega)$ is the *cumulative* control matrix of a sequence of G total steps up to step g and can thus be viewed as a function defined at discrete points in time, $\mathcal{M}^{(g)}(\omega) \simeq \mathcal{M}(\omega; t_0, t_g)$. Finally, we drop the specifier $\mathcal{F}^{(2)}$ distinguishing the second- from the first-order filter function for brevity; in this section, we always mean the former.

In the following, we will consider a sequence of piecewise-constant time steps split up into subsequences and will deal on the one hand with quantities that depend exclusively on the internal structure of a subsequence and those that do not depend on the internal structure on the other. For the former, we will denote their internal time step by a parenthesised superscript, *e.g.* $A^{(i)}$, which means the ith time step of A. The latter will have no superscript as they do not depend on the internal structure. We will furthermore distinguish between *local* quantities, which do not depend on the preceding dynamics (that is, are functions of the subsequence alone), and denote the subsequence index they belong to by a parenthesised subscript, *e.g.* $A_{(i)}$ for some quantity A of sequence i. By contrast, quantities which are *non-local* and thus depend on the preceding dynamics will then be denoted in a "posterior" fashion, *e.g.*, $A_{(i|i-1\to 1)}$ if A is a function of subsequence i and depends on all previous subsequences $i-1, \dots, 1$. A special case is the control propagator up to sequence i, $\mathcal{Q}_{(i-1\to 1)}$, where we drop the index i because the action of $\mathcal{Q}_{(i-1\to 1)}$ during i is the identity operation.

We start from **??**, from which for reasons that will become clear shortly we define the second-order filter function by

$$\mathcal{F}_{\alpha\beta,kl}(\omega) \coloneqq \mathcal{N}_{\alpha\beta,kl}(\omega) + \sum_{g=1}^{G} \mathcal{J}^{(g)}_{\alpha\beta,kl}(\omega) \tag{A.37}$$

with

$$\mathcal{N}_{\alpha\beta,kl}(\omega) \coloneqq \sum_{g=1}^{G} \mathcal{G}^{(g)*}_{\alpha k}(\omega) \mathcal{M}^{(g-1)}_{\beta l}(\omega) \tag{A.37a}$$

$$\mathcal{J}^{(g)}_{\alpha\beta,kl}(\omega) \coloneqq s^{(g)}_{\alpha} \bar{B}^{(g)}_{\alpha,ij} \bar{C}^{(g)}_{k,ji} I^{(g)}_{ijmn}(\omega) \bar{C}^{(g)}_{l,nm} \bar{B}^{(g)}_{\beta,mn} s^{(g)}_{\beta} \tag{A.37b}$$

1: Unfortunately, we are running out of symbols and sticking to our previous convention of using Roman font for Hilbert-space operators and calligraphic font for their Liouville-space duals would lead to naming clashes. We therefore use a calligraphic font for either.

and where repeated indices are contracted. Comparing to the nested time integral, the first summand in the brackets contains all contributions from complete time segments up to the one containing the inner integration variable t, whereas the second captures the final, incomplete segment with $t_{g-1} < t \leq t_g$. Now imagine the sequence of piecewise-constant time steps, $g \in \{1, \dots, G\}$, being split apart at some index $1 < \gamma < G$ and thereby being divided into two subsequences $g \in \{1, \dots, \gamma\}$ and $h \in \{1, \dots, \eta\} \equiv g \in \{\gamma + 1, \dots, G\}$ with $G = \gamma + \eta$. Our goal is to obtain an expression for the second-order filter function $\mathcal{F}(\omega)$ that is – as much as possible – a sum of local terms of these subsequences g and h.

Up to γ, the filter function is simply that of the first sequence, $\mathcal{F}_{(1)}(\omega)$, and we thus have for $g > \gamma$[2]

$$\begin{aligned}\mathcal{F}_{(2|1)}(\omega) &= \mathcal{F}(\omega) - \mathcal{F}_{(1)}(\omega) \\ &= \sum_{g=\gamma+1}^{G} \left[|\mathcal{G}^{(g)}(\omega)\rangle\!\rangle\langle\!\langle \mathcal{M}^{(g-1)}(\omega)| + \mathcal{J}^{(g)}(\omega) \right], \end{aligned} \tag{A.38}$$

2: We drop indices for legibility as stated above; $\mathcal{J}^{(g)}(\omega)$ is a matrix on Liouville space, whereas $\mathcal{G}^{(g)}(\omega)$ and $\mathcal{M}^{(g)}(\omega)$ are Liouville-space row vectors and their product here is an outer product, $|\mathcal{G}^{(g)}(\omega)\rangle\!\rangle\langle\!\langle \mathcal{M}^{(g-1)}(\omega)|$, resulting in a matrix on Liouville space.

where we already plugged in Equation A.37a. We must now express the quantities $\mathcal{G}^{(g)}(\omega)$, $\mathcal{M}^{(g-1)}(\omega)$, and $\mathcal{J}^{(g)}(\omega)$ locally in terms of the index h. To this end, we first write down the step-wise control matrix $\mathcal{G}^{(g)}(\omega)$ in the second sequence and split off phases and propagators from the first sequence,

$$\begin{aligned}\langle\!\langle \mathcal{G}^{(g)}(\omega)| &= e^{i\omega t_g} \langle\!\langle \tilde{\mathcal{B}}^{(g)}(\omega)|\, \mathcal{Q}^{(g-1)} \\ &= e^{i\omega(t_\gamma + t_h)} \langle\!\langle \tilde{\mathcal{B}}^{(h)}_{(2)}(\omega)|\, \mathcal{Q}^{(h-1)}_{(2)} \mathcal{Q}_{(1)} \\ &= e^{i\omega\tau_{(1)}} \langle\!\langle \mathcal{G}^{(h)}_{(2)}(\omega)|\, \mathcal{Q}_{(1)} \\ &= \langle\!\langle \mathcal{G}^{(h)}_{(2|1)}(\omega)| \end{aligned} \tag{A.39}$$

where $\tau_{(1)} = t_\gamma$ and $\mathcal{Q}_{(1)}$ is the control superpropagator of sequence (1). Next, we consider the cumulative control matrix $\mathcal{M}^{(g-1)}(\omega)$. Because in the total sequence it is given by the sum over all $\mathcal{G}^{(g')}(\omega)$ up to $g-1$, we can split off the complete control matrix of the first sequence and express the remainder by summing over $\mathcal{G}^{(h)}_{(2|1)}(\omega)$ from Equation A.39:

$$\begin{aligned}\langle\!\langle \mathcal{M}^{(g-1)}(\omega)| &= \langle\!\langle \tilde{\mathcal{B}}_{(1)}(\omega)| + e^{i\omega\tau_{(1)}} \sum_{h'=1}^{g-1-\gamma} \langle\!\langle \mathcal{G}^{(h')}_{(2)}(\omega)|\, \mathcal{Q}_{(1)} \\ &= \langle\!\langle \tilde{\mathcal{B}}_{(1)}(\omega)| + e^{i\omega\tau_{(1)}} \langle\!\langle \mathcal{M}^{(g-1-\gamma)}_{(2)}(\omega)|\, \mathcal{Q}_{(1)} \\ &= \langle\!\langle \mathcal{M}^{(h-1)}_{(2|1)}(\omega)| \,. \end{aligned} \tag{A.40}$$

Finally, we need to unravel $\mathcal{J}^{(g)}(\omega)$. We start from **??**, consider a time step $g \geq \gamma$ in the second sequence with $h = g - \gamma$, and rewrite

$$\begin{aligned}\mathcal{J}^{(g)}_{kl}(\omega) =& s^{(g)} \bar{B}^{(g)}_{ij} \bar{C}^{(g)}_{kji} I^{(g)}_{ijmn}(\omega) \bar{C}^{(g)}_{(2|1),lnm} \bar{B}^{(g)}_{mn} s^{(g)} \\ =& s^{(h)}_{(2)} \bar{B}^{(h)}_{(2),ij} \bar{C}^{(h)}_{(2|1),kji} I^{(h)}_{(2),ijmn}(\omega) \bar{C}^{(h)}_{(2|1),lnm} \bar{B}^{(h)}_{(2),mn} s^{(h)}_{(2)} \\ =& \mathcal{J}^{(h)}_{(2|1),kl}(\omega) \end{aligned} \tag{A.41}$$

because all quantities except for $\bar{C}^{(g)}_{(2|1)}$ depend on their timestep g alone, and where i, j, m, n index the Hilbert space dimensions of the operators, while k, l are the usual indices for the basis elements and therefore Liouville space dimensions. On that term, we can factor out the propagators

of the first complete sequence,[3]

$$\bar{C}^{(h)}_{(2|1),kij} = \left[V^{(h)\dagger}_{(2)} Q^{(h-1)}_{(2)} Q_{(1)} C_k Q^{\dagger}_{(1)} Q^{(h-1)\dagger}_{(2)} V^{(h)}_{(2)}\right]_{ij}. \tag{A.42}$$

We can now finally put all pieces together and, starting from Equation A.38, plug in Equations A.39 to A.41, so that we obtain[4]

$$\begin{aligned}\mathcal{F}_{(2|1)}(\omega) &= \sum_{h=1}^{\eta}\Big[\, |\mathcal{G}^{(h)}_{(2|1)}(\omega)\rangle\!\rangle\langle\!\langle \mathcal{M}^{(h-1)}_{(2|1)}(\omega)| + \mathcal{J}^{(h)}_{(2|1)}(\omega)\Big] \\ &= \sum_{h=1}^{\eta}\Big\{ e^{-i\omega\tau_{(1)}} Q^{\top}_{(1)} |\mathcal{G}^{(h)}_{(2)}(\omega)\rangle\!\rangle \\ &\qquad \times \left[\langle\!\langle \tilde{\mathcal{B}}_{(1)}(\omega)| + e^{i\omega\tau_{(1)}} \langle\!\langle \mathcal{M}^{(g-1-\gamma)}_{(2)}(\omega)|\, Q_{(1)}\right] + \mathcal{J}^{(h)}_{(2|1)}(\omega)\Big\}.\end{aligned} \tag{A.43}$$

To simplify the unwieldy first summand in the curly braces further, we expand the product,

$$\begin{aligned} & e^{-i\omega\tau_{(1)}} Q^{\top}_{(1)} |\mathcal{G}^{(h)}_{(2)}(\omega)\rangle\!\rangle \left[\langle\!\langle \tilde{\mathcal{B}}_{(1)}(\omega)| + e^{i\omega\tau_{(1)}} \langle\!\langle \mathcal{M}^{(h-1)}_{(2)}(\omega)|\, Q_{(1)}\right] \\ &\quad = e^{-i\omega\tau_{(1)}} Q^{\top}_{(1)} |\mathcal{G}^{(h)}_{(2)}(\omega)\rangle\!\rangle\langle\!\langle \tilde{\mathcal{B}}_{(1)}(\omega)| + Q^{\top}_{(1)} |\mathcal{G}^{(h)}_{(2)}(\omega)\rangle\!\rangle\langle\!\langle \mathcal{M}^{(h-1)}_{(2)}|\, Q_{(1)}. \end{aligned} \tag{A.44}$$

If we now pull in the sum over the time steps h, we can identify the control matrix in the first term and the contribution from complete segments to the second-order filter function ($\mathcal{N}_{(2)}(\omega)$, Equation A.37a) in the second,

$$\begin{aligned} & \sum_{h=1}^{\eta} e^{-i\omega\tau_{(1)}} Q^{\top}_{(1)} |\mathcal{G}^{(h)}_{(2)}(\omega)\rangle\!\rangle\langle\!\langle \tilde{\mathcal{B}}_{(1)}(\omega)| + Q^{\top}_{(1)} |\mathcal{G}^{(h)}_{(2)}(\omega)\rangle\!\rangle\langle\!\langle \mathcal{M}^{(h-1)}_{(2)}|\, Q_{(1)} \\ &\quad = e^{-i\omega\tau_{(1)}} Q^{\top}_{(1)} |\tilde{\mathcal{B}}_{(2)}(\omega)\rangle\!\rangle\langle\!\langle \tilde{\mathcal{B}}_{(1)}(\omega)| + Q^{\top}_{(1)} \mathcal{N}_{(2)}(\omega) Q_{(1)}. \end{aligned} \tag{A.45}$$

As a last step, we recognize that the bra in the first term is nothing else but Equation A.34 so that we can write the filter function succinctly as

$$\begin{aligned}\mathcal{F}_{(2|1)}(\omega) &= |\mathcal{G}_{(2)}(\omega)\rangle\!\rangle\langle\!\langle \tilde{\mathcal{B}}_{(1)}(\omega)| + Q^{\top}_{(1)} \mathcal{N}_{(2)}(\omega) Q_{(1)} + \sum_{h=1}^{\eta} \mathcal{J}^{(h)}_{(2|1)}(\omega) \\ &= \mathcal{N}_{(2|1)}(\omega) + \sum_{h=1}^{\eta} \mathcal{J}^{(h)}_{(2|1)}(\omega). \end{aligned} \tag{A.46}$$

In Equation A.46, all terms except the last are known ahead of time if the first- and second-order filter functions of the subsequences as well as the control matrix of the concatenated sequence have been computed. We can extend this result to sequences consisting of an arbitrary number of G subsequences with lengths $\{\eta_g\}_{g=1}^{G}$ by recursively shifting indices in Equation A.46, (2) → (3), (1) → (2), and adding $\mathcal{F}_{(2|1)}(\omega)$, allowing us to write the concatenation rule for second-order filter functions as

$$\begin{aligned}\mathcal{F}(\omega) &= \sum_{g=1}^{G} \mathcal{F}_{(g|g-1\to 1)}(\omega) \\ &= \sum_{g=1}^{G}\left[\mathcal{N}_{(g|g-1\to 1)}(\omega) + \sum_{h_g=1}^{\eta_g} \mathcal{J}^{(h_g)}_{(g|g-1\to 1)}(\omega).\right] \end{aligned} \tag{A.47}$$

3: Note that the $Q_{(i)}$ here are Hilbert space propagators, not their Liouville space counter parts $\mathcal{Q}_{(i)}$, and that $Q^{(h-1)}_{(1)} \equiv Q_{h-1}$ in the notation of **??**.

4: Recall that $\mathcal{Q}$ is the Liouville representation of the unitary operator Q and as such – and because our chosen basis C is Hermitian – is an orthogonal matrix for which $\mathcal{Q}^{\top}\mathcal{Q} = \mathbb{1}$.

with

$$\mathcal{N}_{(g|g-1\to 1)}(\omega) = |\mathcal{G}_{(g)}(\omega)\rangle\!\rangle\langle\!\langle\tilde{\mathcal{B}}_{(g-1)}(\omega)| + \mathcal{Q}^{\top}_{(g-1\to 1)}\mathcal{N}_{(g)}(\omega)\mathcal{Q}_{(g-1\to 1)} \tag{A.47a}$$

and

$$\mathcal{J}^{(h)}_{(g|g-1\to 1),kl}(\omega) = s^{(h)}_{(g)}\bar{B}^{(h)}_{(g),ij}\bar{C}^{(h)}_{(g|g-1\to 1),kji}I^{(h)}_{(g),ijmn}(\omega)\bar{C}^{(h)}_{(g|g-1\to 1),lnm}\bar{B}^{(h)}_{(g),mn}s^{(h)}_{(g)} \tag{A.47b}$$

Equation A.47 is our final result. Before we analyze it in more detail, let us first briefly discuss the special case where $G = 1$. Then, $\mathcal{Q}_{(0)} = \mathbb{1}$, $\langle\!\langle\tilde{\mathcal{B}}_{(0)}| = 0$, and hence $|\mathcal{G}_{(1)}(\omega)\rangle\!\rangle\langle\!\langle\tilde{\mathcal{B}}_{(0)}(\omega)| = 0$ so that Equation A.46 reduces to Equation A.37 as it should.

Monte Carlo and GKSL master equation simulations

B

B.1 Validation of QFT fidelities

In this section, we perform Gorini-Kossakowski-Sudarshan-Lindblad (GKSL) master equation and Monte Carlo (MC) simulations to verify the fidelities predicted for the QFT circuit in the main text. We focus on noise exclusively on the third qubit, entering through the noise operator $B_\alpha \equiv \sigma_y^{(3)}$.

this

We assemble the QFT circuit discussed in the main text from a minimal gate set consisting of three atomic gates, $\mathbb{G} = \{\mathrm{X}_i(\pi/2), \mathrm{Y}_i(\pi/2), \mathrm{CR}_{ij}(\pi/2^3)\}$ on or between qubits i and j. We consider a simple model involving four single-spin qubits with in-phase (I) and quadrature (Q) single-qubit control and nearest neighbor exchange coupling so that the control Hamiltonian reads

$$H_\mathrm{c}(t) = \sum_{\langle i,j\rangle} I_i(t)\sigma_x^{(i)} + Q_i(t)\sigma_y^{(i)} + J_{ij}(t)\sigma_z^{(i)} \otimes \sigma_z^{(j)} \tag{B.1}$$

where $\sigma_\alpha^{(i)}$ is the trivial extension of the Pauli matrix σ_α of qubit i to the full tensor product Hilbert space. For simplicity, we assume periodic boundary conditions so that qubits 1 and 4 are nearest neighbors as well. Similarly, we define the noise Hamiltonian as

$$H_\mathrm{n}(t) = \sum_{\langle i,j\rangle} b_I(t)\sigma_x^{(i)} + b_Q(t)\sigma_y^{(i)} + b_J(t)\sigma_z^{(i)} \otimes \sigma_z^{(j)} \tag{B.2}$$

with the noise fields $b_\alpha(t)$ for $\alpha \in \{I, Q, J\}$.

To validate the fidelity for white noise, we use a GKSL master equation [7, 8] in superoperator form. We represent linear maps $\mathcal{A} : \rho \to \mathcal{A}(\rho)$ by matrices in the Pauli transfer matrix (PTM) representation as (see Reference 9 for more details)

$$\mathcal{A}_{ij} \coloneqq \mathrm{tr}\Big(\sigma_i \mathcal{A}(\sigma_j)\Big) \tag{B.3}$$

and operators as column vectors (*i. e.*, generalized Bloch vectors) as

$$\rho_i \coloneqq \mathrm{tr}(\sigma_i \rho), \tag{B.4}$$

allowing us to write the Lindblad equation

$$\frac{\mathrm{d}}{\mathrm{d}t}\rho(t) = -i[H(t), \rho(t)] + \sum_\alpha \gamma_\alpha \left(L_\alpha \rho(t) L_\alpha^\dagger - \frac{1}{2}\Big\{L_\alpha^\dagger L_\alpha, \rho(t)\Big\}\right) \tag{B.5}$$

as a linear differential equation in matrix form,

$$\frac{\mathrm{d}}{\mathrm{d}t}\rho_i(t) = \sum_j \left(-i\mathcal{H}_{ij}(t) + \sum_\alpha \gamma_\alpha \mathcal{D}_{\alpha,ij}\right)\rho_j(t). \tag{B.6}$$

Here, $\mathcal{H}_{ij}(t) = \mathrm{tr}\Big(\sigma_i\big[H(t), \sigma_j\big]\Big)$ and $\mathcal{D}_{\alpha,ij} = \mathrm{tr}\Big(\sigma_i L_\alpha \sigma_j L_\alpha^\dagger - \frac{1}{2}\sigma_i\Big\{L_\alpha^\dagger L_\alpha, \sigma_j\Big\}\Big)$. By setting $L_\alpha \equiv \sigma_y^{(3)}$ as well as $\gamma_\alpha \equiv S_0/2$ with S_0 the amplitude of the one-sided noise power spectral density (PSD) so that $S(\omega) = S_0$, we can compare the fidelity obtained from the filter functions to that from the explicit simulation of Equation B.6. The latter is computed as $F_\mathrm{avg} =$

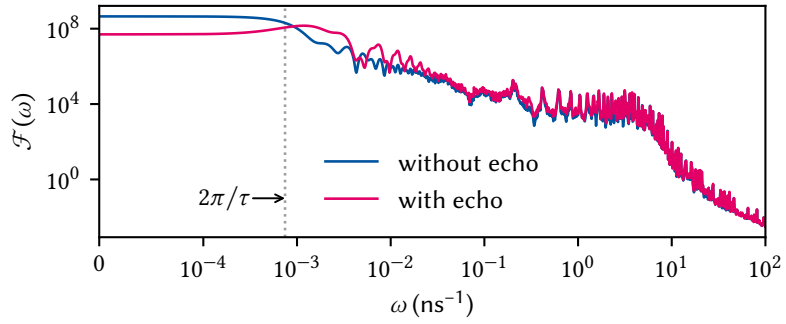

Figure B.1: Filter functions for noise operator $\sigma_y^{(3)}$ for the QFT circuit without (blue) and with (magenta) additional echo pulses. Introducing the echoes shifts spectral weight towards higher frequencies, reducing the DC level of the filter function by two orders of magnitude and thus leading to an improved fidelity for $1/f$ noise.

$d^{-2}\,\mathrm{tr}\left(\mathcal{Q}^\dagger\mathcal{U}\right)$, where $\mathcal{Q}$ is the superpropagator due to the Hamiltonian evolution alone (*i.e.*, the ideal evolution without noise).

For the Monte Carlo simulation, we explicitly generate time traces of $b_Q(t)$ (*cf.* Equation B.2) by drawing pseudo-random numbers from a distribution whose PSD is $S(f) = S_0/f$. To do this, we draw complex, normally distributed samples in frequency space (*i.e.* white noise), scale it with the square root of the PSD, and finally perform the inverse Fourier transform. We choose an oversampling factor of 16 so that the time discretization of the simulation is $\Delta t_{\mathrm{MC}} = \Delta t/16 = 62.5\,\mathrm{ps}$ ($\Delta t = 1\,\mathrm{ns}$ is the time step of the pulses used in the filter function (FF) simulation), leading to a highest resolvable frequency of $f_{\max} = 16\,\mathrm{GHz}$. Conversely, we increase the frequency resolution by sampling a time trace longer by a given factor, giving frequencies below $f_{\min}$ (16 kHz for pink, 0 Hz for white noise) weight zero, and truncating it to the number of time steps in the algorithm times the oversampling factor. This yields a time trace with frequencies $f \in [f_{\min}, f_{\max}]$ and a given resolution (we choose $\Delta f = 160\,\mathrm{Hz}$). For reference, we show the fidelity filter functions for the circuit with and without echo pulses in this frequency band in Figure B.1.

We then proceed to diagonalize the Hamiltonian $H(t) = H_c(t) + H_n(t)$ and compute the propagator for one noise realization as

$$U(t) = \prod_g V^{(g)} \exp\left(-i\Omega^{(g)}\Delta t_{\mathrm{MC}}\right) V^{(g)\dagger}, \tag{B.7}$$

where $V^{(g)}$ is the unitary matrix of eigenvectors of $H(t)$ during time segment g and $\Omega^{(g)}$ the diagonal matrix of eigenvalues. Finally, we obtain an estimate for the average gate fidelity F_{avg} from the entanglement fidelity F_{ent} as

$$\left\langle F_{\mathrm{avg}}\right\rangle = \left\langle \frac{dF_{\mathrm{ent}} + 1}{d+1}\right\rangle = \left\langle \frac{\left|\mathrm{tr}\left(Q^\dagger U(\tau)\right)\right|^2 + d}{d(d+1)}\right\rangle. \tag{B.8}$$

Here, $Q \equiv U_{\mathrm{c}}(t=\tau)$ is the noise-free propagator at time τ of completion of the circuit and $\langle\,\bullet\,\rangle$ denotes the ensemble average over N Monte Carlo realizations of Equation B.7, *i.e.*, $\langle A\rangle = N^{-1}\sum_{i=1}^{N} A_i$. The standard error of the mean can be obtained as $\sigma_{\langle F_{\mathrm{avg}}\rangle} = \sigma_{F_{\mathrm{avg}}}/\sqrt{N}$ with $\sigma_{F_{\mathrm{avg}}}$ the standard deviation over the Monte Carlo traces.

Table B.1 compares the infidelities $I = 1 - F$ from GKSL and MC simulations to the filter function predictions following **??**. Note that the precise value of the filter function result depends quite sensitively on the frequency sampling due to the sharp peaks in the gigahertz range (Figure B.1). As the table shows, both the GKSL and the MC calculations agree well with the predictions made by our filter-function formalism.

Table B.1: Infidelities $I_{\text{avg}} = 1 - F_{\text{avg}}$ of the QFT circuit due to noise on $\sigma_y^{(3)}$. MC values are averages over $N = 1000$ random traces and have a relative error of 3 %. We included frequencies in the range of $\omega \in [0, 100]\,\text{ns}^{-1}$ for white noise, and $\omega \in [100\,\text{ms}^{-1}, 100\,\text{ns}^{-1}]$ for pink noise. FF values are computed with $n_\omega = 1000$ samples logarithmically distributed over the same interval. Prefactors in the power law $S(\omega) = A\omega^\alpha$ are $2 \times 10^{-6}\,\text{ns}^{-1}$ and $10^{-9}\,\text{ns}^{-2}$, respectively.

	White noise		$1/f$ noise	
Method	Without echo	With echo	Without echo	With echo
GKSL	8.38×10^{-3}	8.38×10^{-3}	—	—
MC	8.74×10^{-3}	8.00×10^{-3}	2.11×10^{-2}	4.28×10^{-3}
FF	8.38×10^{-3}	8.40×10^{-3}	2.12×10^{-2}	4.46×10^{-3}

Bibliography

[1] Łukasz Cywiński et al. "How to Enhance Dephasing Time in Superconducting Qubits." In: *Physical Review B* 77.17 (May 13, 2008), p. 174509. DOI: 10.1103/PhysRevB.77.174509 (cited on page 9).

[2] Pascal Cerfontaine et al. "Closed-Loop Control of a GaAs-based Singlet-Triplet Spin Qubit with 99.5% Gate Fidelity and Low Leakage." In: *Nature Communications* 11.1 (Dec. 2020), p. 4144. DOI: 10.1038/s41467-020-17865-3 (cited on pages 9, 10).

[3] Christopher J. Wood and Jay M. Gambetta. "Quantification and Characterization of Leakage Errors." In: *Physical Review A* 97.3 (Mar. 8, 2018), p. 032306. DOI: 10.1103/PhysRevA.97.032306 (cited on page 9).

[4] J. R. Johansson, P. D. Nation, and Franco Nori. "QuTiP: An Open-Source Python Framework for the Dynamics of Open Quantum Systems." In: *Computer Physics Communications* 183.8 (Aug. 1, 2012), pp. 1760–1772. DOI: 10.1016/j.cpc.2012.02.021 (cited on page 11).

[5] Todd J. Green et al. "Arbitrary Quantum Control of Qubits in the Presence of Universal Noise." In: *New Journal of Physics* 15.9 (Sept. 12, 2013), p. 095004. DOI: 10.1088/1367-2630/15/9/095004. arXiv: 1211.1163 (cited on pages 11, 13).

[6] P C Moan, J A Oteo, and J Ros. "On the Existence of the Exponential Solution of Linear Differential Systems." In: *Journal of Physics A: Mathematical and General* 32.27 (1999), pp. 5133–5139. DOI: 10.1088/0305-4470/32/27/311 (cited on page 11).

[7] G. Lindblad. "On the Generators of Quantum Dynamical Semigroups." In: *Communications in Mathematical Physics* 48.2 (June 1976), pp. 119–130. DOI: 10.1007/BF01608499 (cited on page 18).

[8] Vittorio Gorini, Andrzej Kossakowski, and E. C. G. Sudarshan. "Completely Positive Dynamical Semigroups of N-level Systems." In: *Journal of Mathematical Physics* 17.5 (1976), p. 821. DOI: 10.1063/1.522979 (cited on page 18).

[9] Tobias Hangleiter, Pascal Cerfontaine, and Hendrik Bluhm. "Filter-Function Formalism and Software Package to Compute Quantum Processes of Gate Sequences for Classical Non-Markovian Noise." In: *Physical Review Research* 3.4 (Oct. 18, 2021), p. 043047. DOI: 10.1103/PhysRevResearch.3.043047 (cited on page 18).

Special Terms

D
DCG dynamically corrected gate. 10

F
FF filter function. 19, 20

G
GGM generalized Gell-Mann. 10
GKSL Gorini-Kossakowski-Sudarshan-Lindblad. iii, 18–20
GRAPE gradient ascent pulse engineering. iii, 6, 10, 11

I
IQ in-phase/quadrature. 10

M
MC Monte Carlo. 18–20
ME Magnus expansion. 11–13

P
PSD power spectral density. 18, 19
PTM Pauli transfer matrix. 18

Q
QFT quantum Fourier transform. iii, 6, 10, 18–20

Declaration of Authorship

I, Tobias Hangleiter, declare that this thesis and the work presented in it are my own and has been generated by me as the result of my own original research.

I do solemnly swear that:

1. This work was done wholly or mainly while in candidature for the doctoral degree at this faculty and university;
2. Where any part of this thesis has previously been submitted for a degree or any other qualification at this university or any other institution, this has been clearly stated;
3. Where I have consulted the published work of others or myself, this is always clearly attributed;
4. Where I have quoted from the work of others or myself, the source is always given. This thesis is entirely my own work, with the exception of such quotations;
5. I have acknowledged all major sources of assistance;
6. Where the thesis is based on work done by myself jointly with others, I have made clear exactly what was done by others and what I have contributed myself;
7. Parts of this work have been published before as:

[1] Pascal Cerfontaine, Tobias Hangleiter, and Hendrik Bluhm. "Filter Functions for Quantum Processes under Correlated Noise." In: *Physical Review Letters* 127.17 (Oct. 18, 2021), p. 170403. DOI: 10.1103/PhysRevLett.127.170403.

[2] Thomas Descamps, Feng Liu, Tobias Hangleiter, Sebastian Kindel, Beata E. Kardynał, and Hendrik Bluhm. "Millikelvin Confocal Microscope with Free-Space Access and High-Frequency Electrical Control." In: *Review of Scientific Instruments* 95.8 (Aug. 9, 2024), p. 083706. DOI: 10.1063/5.0200889.

[3] Tobias Hangleiter, Pascal Cerfontaine, and Hendrik Bluhm. "Filter-Function Formalism and Software Package to Compute Quantum Processes of Gate Sequences for Classical Non-Markovian Noise." In: *Physical Review Research* 3.4 (Oct. 18, 2021), p. 043047. DOI: 10.1103/PhysRevResearch.3.043047.

Aachen, September 4, 2025.